11th ANKARA INTERNATIONAL AEROSPACE CONFERENCE **AIAC-2021-117**
8-10 September 2021 - METU, Ankara TURKEY

AERODYNAMIC ANALYSIS OF FLOW AROUND APOLLO REENTRY CAPSULE USING SU2 COUPLED WITH AN ANISOTROPIC MESH ADAPTATION

Badamasi Babaji[1]
Istanbul Technical University
Istanbul, Turkey

Mehmet Sahin[2]
Istanbul Technical University
Istanbul, Turkey

ABSTRACT

During the reentry phase, the earth atmosphere represents a relatively dense fluid medium and a reentry vehicle has to follow a very narrow re-entry corridor in order to have a safe landing. If the vehicle strays above the corridor, it may skip out and back to the cold space environment. If it strays below the corridor, it may burn up and/or experience excessive g-force. The objective of this paper is numerical investigation of the flow field around Apollo AS-202 reentry capsule using open source CFD solver, SU2 coupled with anisotropic mesh refinement library pyAMG. The simulations are performed at various angle of attacks, Mach and Reynold's number. The results have shown a fair agreement between the computational method and experimental data. A shadowgraph comparison has demonstrated some experimentally observed features of the flow field like bow shock, shear layers and reattachment regions.

INTRODUCTION

Atmospheric reentry is the movement of space vehicle from the cold environment of outer space into the atmospheric envelope of a planet. During the reentry, the atmosphere poses as an obstacle wall made of dense fluid. Astronauts most attempt to enter the atmosphere at the correct angle and speed in order to avoid fatal accident. Reentry capsules are designed with a blunt body to survive the extreme aerodynamic conditions. Understanding the flow field around the capsule is very important to engineers and designers for the design of such vehicles. Recently, astronomical missions are gaining global recognition as mankind continues its mission of moving to outer space. The results from the numerical and experimental analysis are vital in designing the thermal protections system (TPS), including material selection and integration which considerably affect the total mass of the reentry capsule. Computational fluid dynamics (CFD) has recently been used extensively to simulate flow at supersonic speed as these flow conditions are difficult and expensive to replicate in wind and shock tunnels [Shafeeque, 2017]. The use of CFD to understand the flow field at such conditions is much more economical and therefore is used extensively by researchers and engineers as an analysis tool to understanding the complicated hypersonic flow conditions [Mathews, 2015].

[1] M.Sc student, Aeronautical and Astronautical engineering, Email: babaji18@itu.edu.tr
[2] Prof. of Aeronautical and Astronautical engineering, Email: msahin@itu.edu.tr

In literature, there are several papers that investigated numerical the flow field around the Apollo capsule focusing on different aspect of the flow. The study by [Sinha & Dey, 2010] focused on the afterbody flow field, they used CFD to reaffirm the experimental phenomena of the local flow separation and reattachment on the windward meridian at selected angle of attack. A similar study with a capsule of different geometry was carried out by [Schrijer & Walpot, 2010]. The objective of the current study is to use computational fluid dynamics to simulate the flow field conditions and validate the results with experimental data. To Improve the solution accuracy and reduce the convergence time, mesh adaptation library pyAMG [Alauzet & Loseille, 2016] is coupled to the open-source CFD solver, SU2 [Economon et al., 2016, p. 2].

GOVERNING EQUATIONS

The governing equation for the flow analysis is the compressible Navier Stokes equations which can be written in conservative integral form as:

$$\frac{\partial}{\partial t}\int_{\Omega} \boldsymbol{Q} dV + \oint_{\partial\Omega} \boldsymbol{n}.\boldsymbol{F_i} dS - \oint_{\partial\Omega} \boldsymbol{n}.\boldsymbol{F_v} dS = 0 \quad (1)$$

For a vertex based finite volume solver, the residual vector can be written as:

$$\boldsymbol{R}(\boldsymbol{Q}) = \frac{\partial}{\partial t}\int_{\Omega} \boldsymbol{Q} dV + \oint_{\partial\Omega} n.\boldsymbol{F_i} dS - \oint_{\partial\Omega} n.\boldsymbol{F_v} dS = 0 \quad (2)$$

Equation (1) is the integral form of the compressible Navier-Stokes's equation and it is the governing equation for the current analysis. If the last term in equation (1) is ignored, the equation becomes the inviscid Euler equation. The spalart-Allmaras one equation turbulence model is used in order to account for turbulence effects.

METHODOLOGY

Compressible Euler equation is solved for a simple case of hypersonic flow over a unit cylinder at Mach 6 where the fluid medium is assumed to be a perfect gas. Additionally, compressible Navier-Stokes's equation is solved with Spalart-Allmaras turbulence model for the flow over Apollo AS-202 reentry capsule. The simulation is normalized with freestream velocity equals to Mach number for simplicity as our interest is accurately capturing the shock regions and other physical phenomenon and at the same time compute the non-dimensional lift and drag coefficients. A constant Courant-Friedrichs-Lewy number (CFL) of 1 is used for the simulations. It is observed that the simulation diverged for a high CFL number. The simulation is carried at various angle of attacks, Mach and Reynold's number. The fluid medium is assumed to be perfect gas for all simulation in this paper. Green-Gauss theorem is used for gradient computations. For the time integration, Newton method with Euler implicit is used for the numerical integration, FGMRES is used for solving the linear system with ILU preconditioner.

GEOMETRY

The geometry of the Apollo AS-202 is shown in Figure 1. It is a blunt forebody with a radius of curvature of 4.694m and a shoulder radius is 0.196m which approximately 10% of the radius of the body. The afterbody is blunted with an angle of inclination of 33 degrees, and 0.231 radius at the end of the capsule. The capsule has a diameter of 3.91m and total axial length of 3.431 which includes the thermal protection system material [Wright et al., 2006]. The capsule is modelled in CAD software and shown in Figure 1.

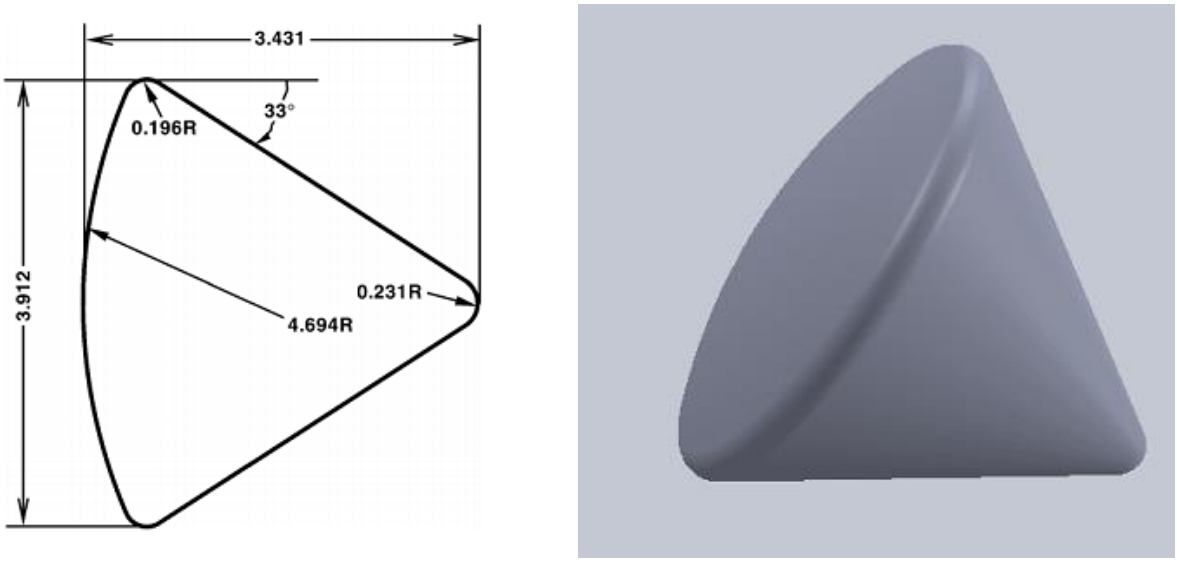

Figure 1: Geometry of Apollo AS-202 reentry capsule.

MESHING

In this study, the computational domain for the Apollo capsule analysis is a sphere with a radius of 50*R* with the Apollo capsule at the center. The initial mesh has 101,233 points and 554,321 unstructured tetrahedral cells. Figure 2 shows the spherical computational domain.

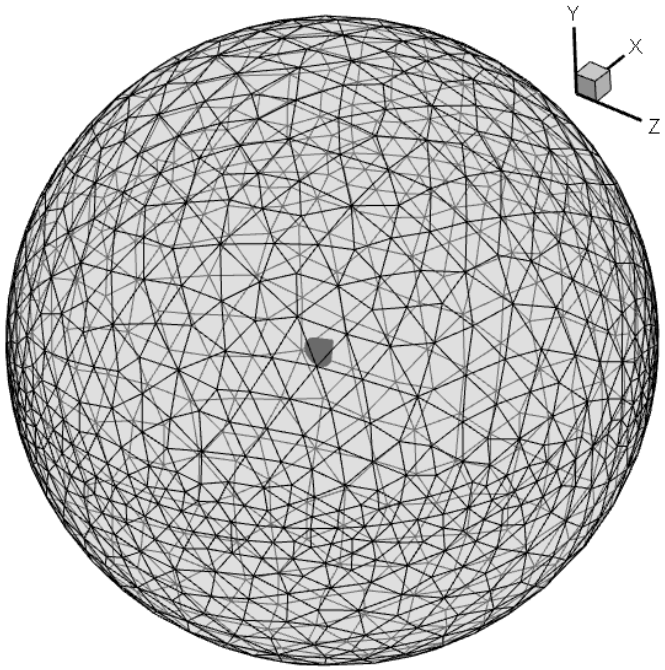

Figure 2: Computational domain for the simulation.

SIMULATION FREESTREAM CONDITIONS

Aerodynamic characteristic of a blunt capsule is important in terms of planning trajectory points and thermal protection system. Aerodynamic performance is evaluated in terms of lift to drag ratio (CL/CD). The goal of this section is to use computational fluid dynamics to simulate the flow conditions and compare the results with experimental data. The selected freestream conditions for the present analysis are given in Table 1.

Table 1: The selected freestream conditions for numerical simulations.

Geometry	Governing equation	Mach number	Reynold's number	Angle of attack
Unit cylinder	Euler	6.0	--	0.0
Apollo AS-202 capsule	RANS	2.98	1.67×10^7	-10 to 180
		10.18	2.45×10^7	0.0

RESULTS

Hypersonic Flow Over a Cylinder.

The inviscid Euler equation is solved around a unit cylinder at hypersonic flow of Mach 6. Figure 3 and 4 gives the comparison of the solution using SU2 in present study in comparison to the shock-fitting by [Salas & Atkins, 2009] and the solution obtained using the space-time conservation element solution element (CESE) method by [Chang, 2007]. The comparison has shown good agreement between these methods and SU2 solver used in present study.

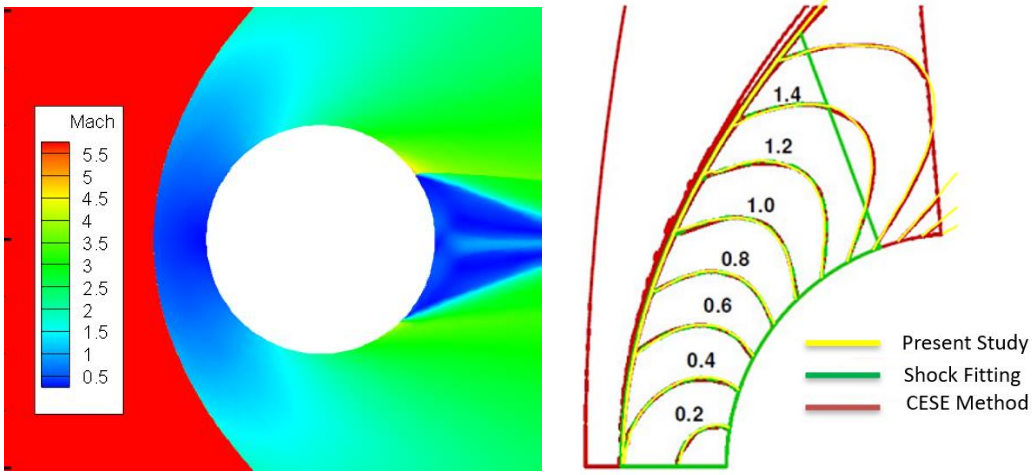

Figure 3: Comparison Mach number contour level obtained in present study vs Shock-fitting and CESE Methods.

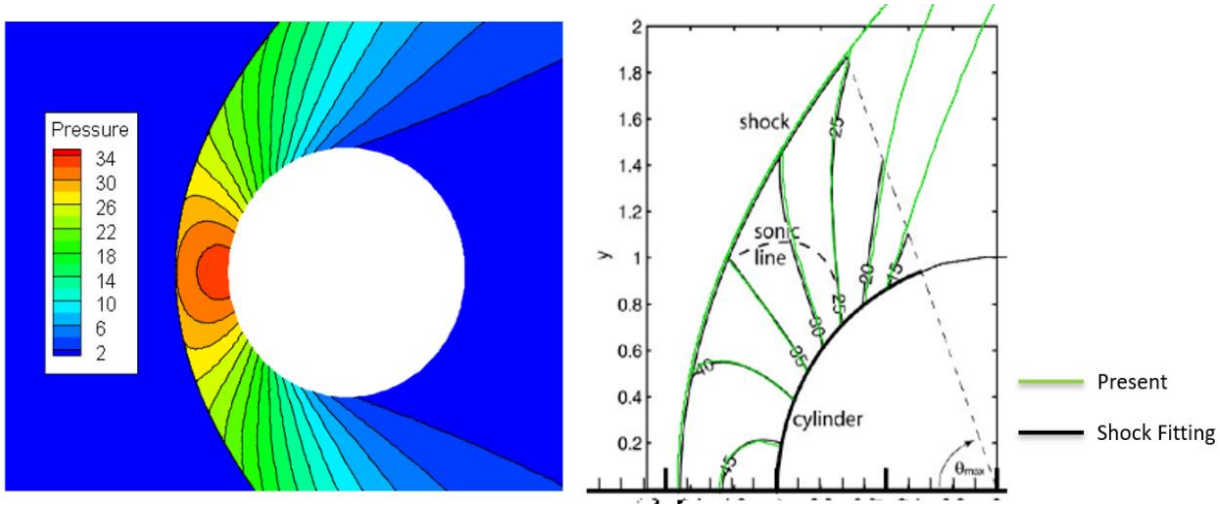

Figure 4: Comparison of Mach number contour level obtained in present study vs Shock-fitting.

Flow Over Apollo AS-202 Reentry Capsule

Figure 5 shows the comparison of the normalized pressure obtained by solving the governing Navier-Stokes equation at Mach number of 10.18 and Reynold's number of 2.45 x 10^7 around Apollo capsule at zero angle of attack. The experimental data for the comparison was obtained from the Apollo wind tunnel experiment [Bertin, 1966].

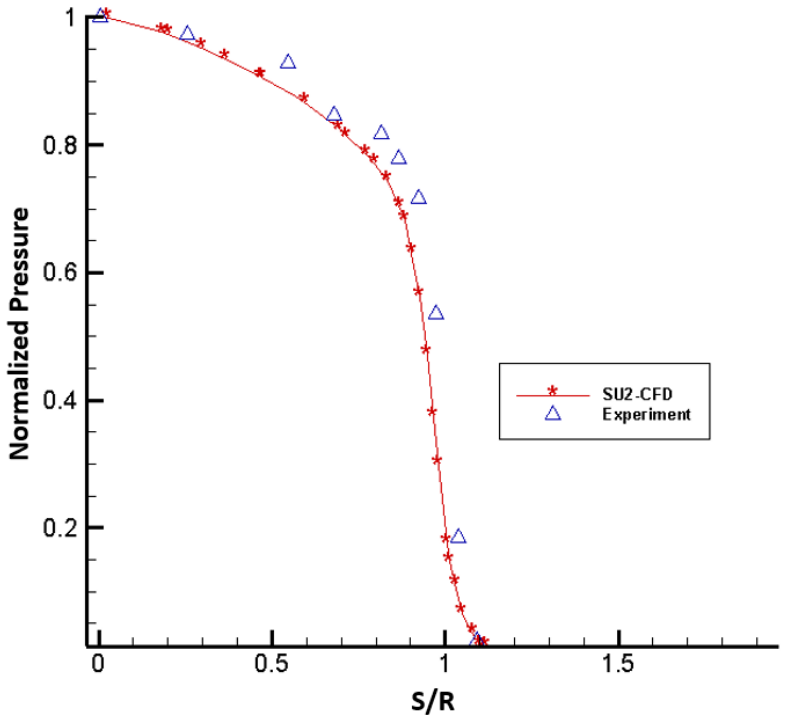

Figure 5: Comparison of normalized pressure along upper half body nose of Apollo As-202 reentry capsule in present study vs experimental for Mach = 10.18 and angle of flow = 0°.

The *S* in the diagram represents the distance along surface from geometric center of spherical heat shield and *R* is maximum body radius of the capsule. Figure 6 shows a good agreement of aerodynamic lift and drag force coefficients in present study vs experimental data [Griffith & Boylan, 1968].

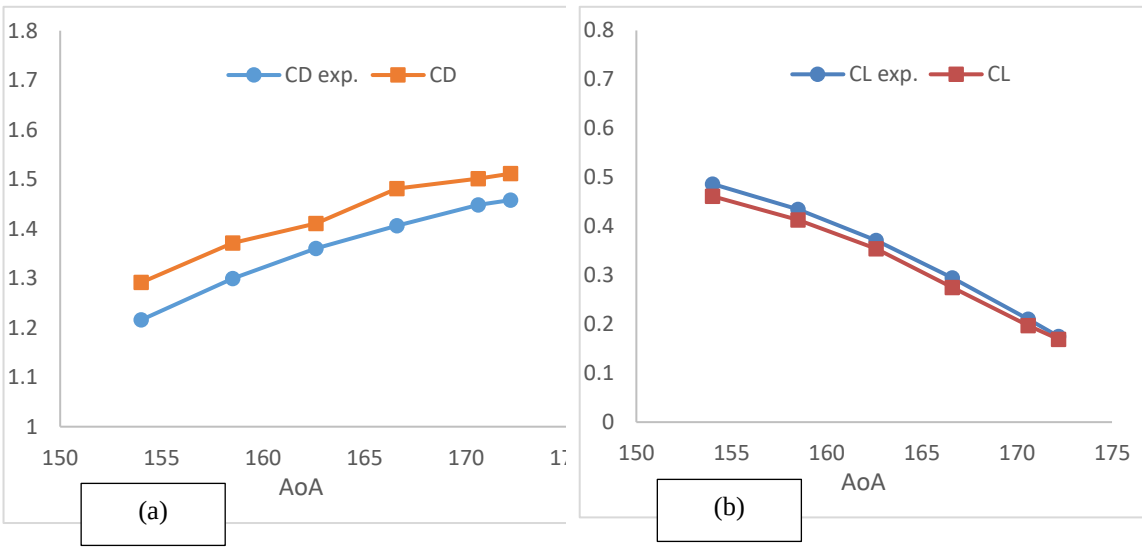

Figure 6: Comparison of drag (a) and lift (b) force coefficients of Apollo reentry capsule at Mach = 2.98 in present simulation vs experimental data.

The flow field contour for the simulation at various angle of attack is shown and explained below. Figure 7 shows the normalized Mach number and pressure contours for flow over Apollo capsule at Mach 2.98 where the flow angle of attach is zero while Figure 8 show flow field at -20^{o} angle of attack.

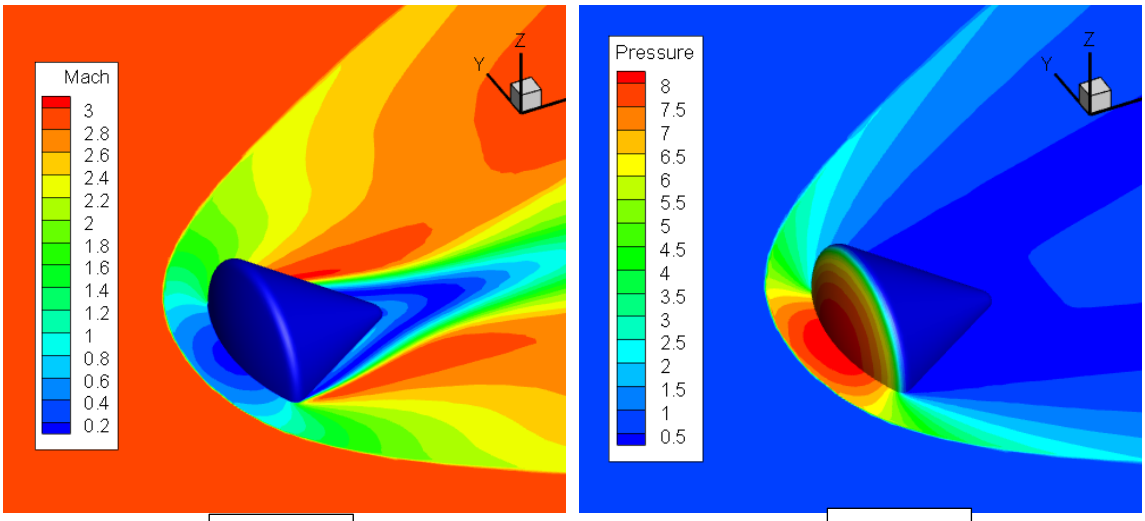

Figure 7: The Mach number (a) and pressure (b) contour distributions around Apollo AS-202 reentry capsule at Mach number = 2.98, angle of flow = 0^{o}.

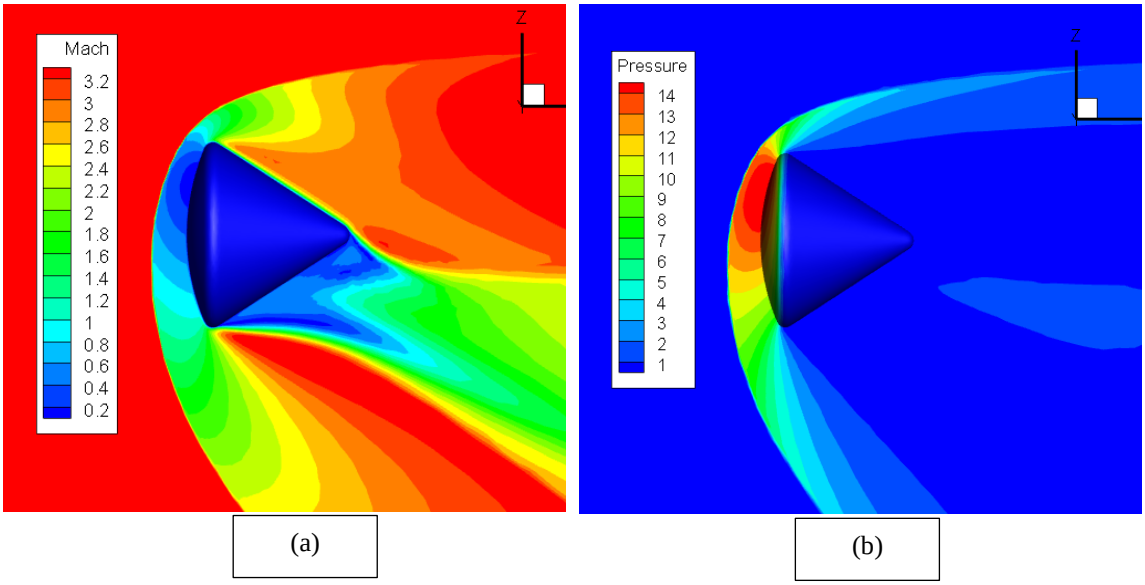

Figure 8: The Mach number (a) and pressure contour (b) distributions around Apollo AS-202 reentry capsule at Mach number = 2.98, Angle of flow = -20^{o}.

At the reentry phase, a strong detached shockwave is observed in front of the reentry capsule. The region afterward the shockwave, a shock layer characterized with high enthalpy and temperature is observed once again, resulting in a severe heating environment around the capsule as seen in Figure 7 and 8. A bow shock formed ahead of the vehicle slows down the hypersonic flow. In a hypersonic regime, nondimensional variables such as lift, drag and pressure coefficient, and flow field structure become Mach number independent. This is the idea behind the Mach number independence hypothesis for hypersonic flow [Anderson, 2009]. Figure 9 shows a typical flow field where the windward free shear layer can be seen to curve around and reattached on the conical frustum. The geometry from the experiments has a more

shaped corners than the Apollo AS-202 capsule modelled in the current CFD analysis. This resulted to a minor change between the two images where the geometry from the simulations produced a more severe circulations behind the capsule.

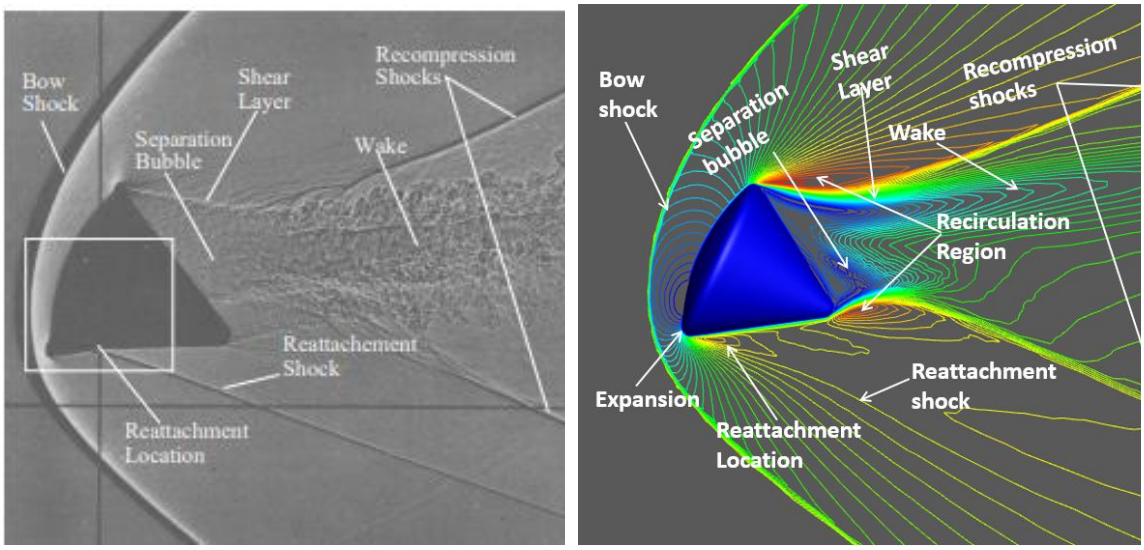

Figure 9: Experimental shadowgraph (a) depicting salient features in the flow around an Apollo- shaped body at Mach 2.2 and angle of attack of 25 deg [Kruse, 1968] vs the result obtained using CFD (b) at the same conditions in the present study.

The streamlines patterns are important to see the nature of the flow path around the capsule. Figure 10 shows the streamlines pattern on the body surface of Apollo AS-202 capsule at Mach 2.98 flow where the angle of attack is 10^{o}.

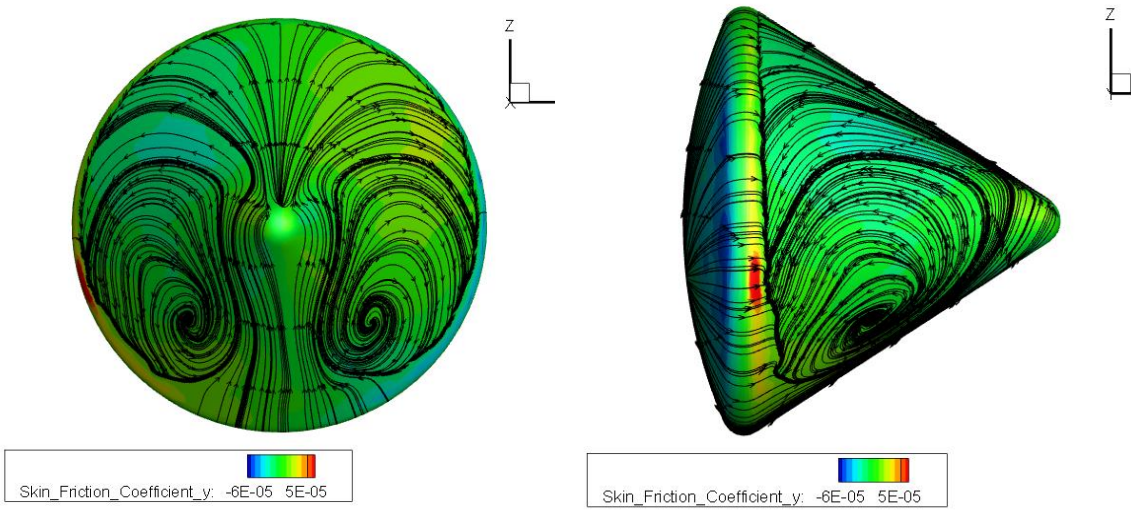

Figure 10: The Streamlines distribution surface skin friction around Apollo AS-202 Reentry capsule at Mach number = 2.98, Angle of flow = 10^{o}.

Flow solutions were computed by solving Navier-Stokes's equation with Spalart-allmaras turbulence model. For all the simulation described in this paper, mesh adaptation is used to improve the accuracy in capturing some salient flow features which is important. The goal of this mesh adaptation is to accurately capture the shocks around the apollo reentry capsule, by creating anisotropic mesh elements along the shocks' directions of anisotropy and reducing the simulation convergence time. The sensor for the current study is the Mach number after a modification to the default setting to ensure that the boundary layer mesh where the Mach gradients are weaker such as separation points are not lost during the refinement.

Table 2: Anisotropic mesh adaptation summary for flow over Apollo AS-202 Reentry capsule.

Refinement Level	Number of vertices	Number of Elements	Number of surfaces elements
	Mach = 2.98, AoA = 0.0		
Initial mesh	101,221	589,066	4,311
Iteration 1	209,215	682,542	4,866
Iteration 2	309,227	782,542	5,126
Iteration 3	511,758	951,333	6,243
Iteration 4	930,983	2,189,292	7,012
Iteration 5	1,301,845	3,199,430	8,185
	Mach = 2.98, AoA = 10		
Initial mesh	102,233	519,055	4,318
Iteration 1	209,213	682,542	4,926
Iteration 2	309,213	782,542	5,326
Iteration 3	533,754	941,233	6,146
Iteration 4	930,983	2,301,362	7,431
Iteration 5	1,291,123	3,211,410	8,985
	Mach = 10.18 AoA = 0.0		
Initial mesh	123,234	548,548	4,218
Iteration 1	217,242	672,842	5,066
Iteration 2	311,214	792,452	5,886
Iteration 3	527,658	952,237	6,244
Iteration 4	940,983	2,189,292	8,012
Iteration 5	1,321,845	3,517,420	10,115

The computed aerodynamics CD, CL, are shown in Figure 11 and 12 respectively, plotted against $N^{-2/3}$ where N is the number of nodes in the mesh. This assumes that the characteristic length of the mesh, h, varies with the inverse of the cube root of the number of nodes, $h \approx N^{-1/3}$. The discretization scheme is also assumed to be second order, so that the computed outputs should vary linearly with h^2.

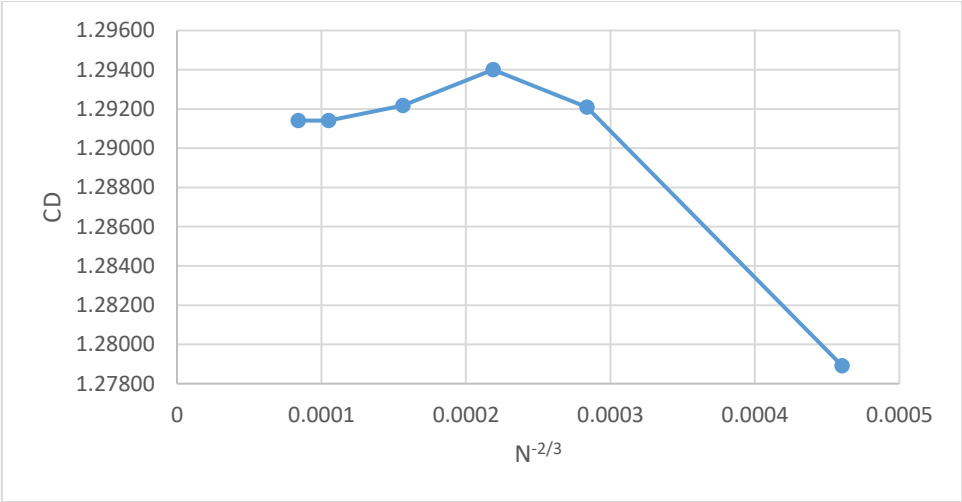

Figure 11: Grid convergence of drag coefficient flow over Apollo-AS-202 reentry capsule at Mach 2.98 and angle of attack 154.

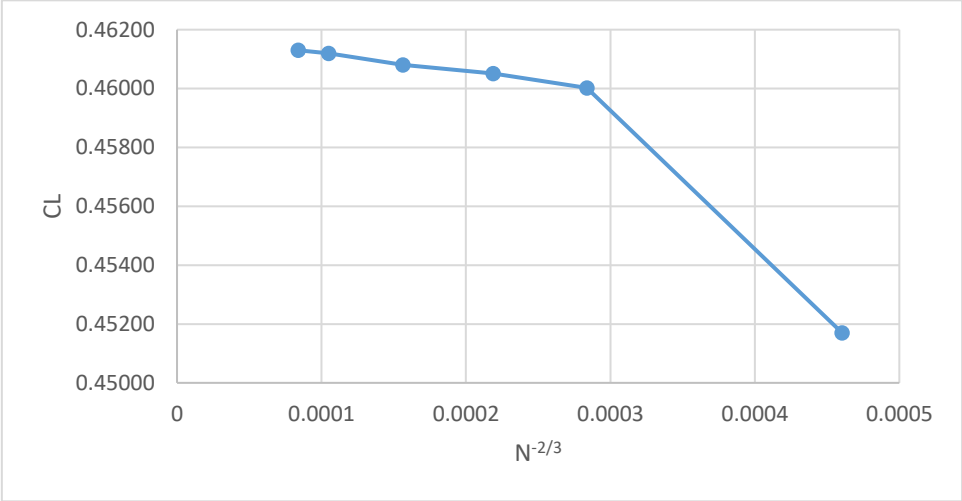

Figure 12: Grid convergence of lift coefficient flow over Apollo-AS-202 reentry capsule at Mach 2.98 and angle of attack 154.

The change in the force coefficient between the initial mesh and the first adapted mesh results observed in Figures 11 and 12 as a result of the drastic change in the distribution of points between the initial and first adapted mesh.

1. CONCLUSION

A detailed analysis of flow around blunt bodies has been carried out using SU2 coupled with solution based anisotropic mesh adaptation software, pyAMG. The fluid model was assumed to be ideal gas, and the parameters of interest were the aerodynamic force coefficients, surface pressure and flow field characteristics. The study has shown a fairly good agreement of the present approach with other numerical and experiment data. The shadowgraph comparison has demonstrated the ability of CFD to capture salient flow features in the flow around an Apollo- shaped body as predicted from wind tunnel experiments. For future analysis, thermal non-equilibrium, and chemical reactions need to be taken into account (SU2-NEMO) to fully understand the effect of these flow properties on the accuracy of the solution.

References

Alauzet, F., & Loseille, A. (2016). A decade of progress on anisotropic mesh adaptation for computational fluid dynamics. *Computer-Aided Design*, *72*, 13–39. https://doi.org/10.1016/j.cad.2015.09.005

Anderson, J. D. (2009). *Fundamentals of Aerodynamics*. 1131.

Bertin, J. J. (1966). *The effect of protuberances, cavities, and angle of attack on the wind-tunnel pressure and heat-transfer distribution for the Apollo command module*. National Aeronautics and Space Administration.

Chang, C.-L. (2007, July 8). Three-Dimensional Navier-Stokes Calculations Using the Modified Space-Time CESE Method. *43rd AIAA/ASME/SAE/ASEE Joint Propulsion Conference & Exhibit*. 43rd AIAA/ASME/SAE/ASEE Joint Propulsion Conference & Exhibit, Cincinnati, OH. https://doi.org/10.2514/6.2007-5818

Economon, T. D., Palacios, F., Copeland, S. R., Lukaczyk, T. W., & Alonso, J. J. (2016). SU2: An Open-Source Suite for Multiphysics Simulation and Design. *AIAA Journal*, *54*(3), 828–846. https://doi.org/10.2514/1.J053813

Griffith, B. J., & Boylan, D. E. (1968). Postflight Apollo command module aerodynamic simulation tests. *Journal of Spacecraft and Rockets*, *5*(7), 843–848.

Kruse, R. L. (1968). *Transition and flow reattachment behind an Apollo-like body at Mach numbers to 9*.

Mathews, D. R. N. (2015). *HYPERSONIC FLOW ANALYSIS ON AN ATMOSPHERIC RE-ENTRY MODULE*. *3*(5), 11.

Salas, M. D., & Atkins, H. L. (2009). On problems associated with grid convergence of functionals. *Computers & Fluids*, *38*(7), 1445–1454.

Schrijer, F., & Walpot, L. (2010). Experimental investigation of the supersonic wake of a reentry capsule. *48th AIAA Aerospace Sciences Meeting Including the New Horizons Forum and Aerospace Exposition*, 1251.

Shafeeque, A. P. (2017). CFD analysis on an atmospheric re-entry module. *International Research Journal of Engineering and Technology*, *4*(01).

Sinha, K., & Dey, A. (2010). Simulation of flow separation and reattachment on a re-entry capsule afterbody frustum. *48th AIAA Aerospace Sciences Meeting Including the New Horizons Forum and Aerospace Exposition*, 1561.

Wright, M. J., Prabhu, D. K., & Martinez, E. R. (2006). Analysis of Apollo Command Module Afterbody Heating Part I: AS-202. *Journal of Thermophysics and Heat Transfer*, *20*(1), 16–30. https://doi.org/10.2514/1.15873